Expanding the PIV Spectral Range and the Turbulence Generated by Grid of Prismatic Circular Cylinders

Daniel Duda[1,*], *Vitalii* Yanovych[1,2], and *Václav* Uruba[1,2]

[1]Faculty of Mechanical Engineering, University of West Bohemia, 306 14 Pilsen, Czech Republic
[2]Instituta of Thermomechanics, Czech Academy of Sciences, 180 00 Prague, Czech Republic

Abstract. The grid turbulence past a grid made of row of prismatic circular rods (rod diameter = 10 mm, rod spacing = 20 mm) perpendicular to the flow is observed by using a pair of PIV cameras. The first one has field of view larger (81 mm), the second one smaller (31 mm), which increases the dynamical range, where the spectral turbulence properties can be explored. Energy spectra displays usual behavior approximately following $k^{-5/3}$ law, the anisotropy originates at larger scales and the flatness describing strong rare events is connected with smaller scales. The spectral properties of vorticity do not collapse due to the different lengthscale of differentiation, which make questionable the previous research based on the vorticity statistics.

Research background: Grid turbulence is the best experimentally accessible prototype of ideal homogenous and isotropic turbulence, although it is known, it is not exactly the ideal one.
Purpose of the article: This contribution explores the possibility of expanding the limited dynamical range of PIV method.
Methods: Particle Image Velocimetry is based on observing the motion of small particles carried by the flow.
Findings & Value added: Anisotropy connected with large scales, flatness with small scales; it does not work for vorticity.

Keywords: Particle Image Velocimetry; Grid turbulence; Spectrum; Anisotropy; Flatness

1 Introduction

Experimental investigation of turbulence is nowadays based on two complementary methods: Hot Wire Anemometry (HWA, or CTA – constant temperature anemometry) and the Particle Image Velocimetry (PIV) [1]. HWA is a very accurate point method with very large dynamical range spanning 5 or more orders of magnitude. PIV is a planar method observing directly the flow structures, but its dynamical range is limited by the size of field of view (FoV) on one side and by the resolution of grid of interrogation areas on the other side. This range is typically 1 : 64 in dependence on the camera resolution and velocity vector

* Corresponding author: dudad@kke.zcu.cz

detection settings. In this contribution we try to enlarge this range by observing the same flow by using two cameras with different FoVs.

2 Methods

2.1 Wind tunnel

The open low-speed wind tunnel is described in our previous work [1]. Its deformation during running are checked [2] by using fast 3D optical scanner Aramis [3]. The wind tunnel test section has dimensions 740 × 300 × 200 mm. In the inlet to the test section there is located a grid of vertical rods (note that grids for turbulence research are mostly realized as a square grids [4], although different shapes and topologies are studied as well, e.g. fractal grids [5]). Despite the prismatic geometry, the flow is expected to be fully 3D as proved by Williamson [6] in the case of a single cylinder. The rods have diameter of d = 10 mm and its distance is M = 20 mm (also referred as Mesh parameter). The tunnel is operated at two velocities 4 m/s and 40 m/s in this case. The corresponding Reynolds numbers based on mesh parameter M are

$$Re_M = \frac{u_{\mathrm{ref}} M}{\nu} = \begin{cases} 5.3 \cdot 10^3 \\ 5.3 \cdot 10^4 \end{cases} \tag{1}$$

later referred just as “lower” and “higher” Re respectively.

2.2 PIV setup

The turbulent flow is measured by using Particle Image Velocimetry (PIV) [7] apparatus, which consists of a pair of FlowSense Mk II cameras, a solid-state Nd:YAG double-pulse laser and a synchronization device. Everything is supplied by the Dantec company. The seeding particles are generated by using fog generator Safex. The Fields of View (FoV) are located within a plane perpendicular to the axes of the rods. The FoV size is different for each camera (see Fig. 1), the larger FoV has size of 81 mm, i.e. 4 × M, while the smaller FoV has size of 31 mm, i.e. 1.5 × M. The smaller FoV is located inside the larger one, both centered approximately at the distance of 235 mm, i.e. aprox. 12 × M from the mesh plane (note the ruler photographed in Fig. 1 has a 10 mm starting length plus the radius of the rods).

(a) Calibration snapshot from 1st cam. (b) Calibration snapshot from 2nd cam. (c) Mapping both figures

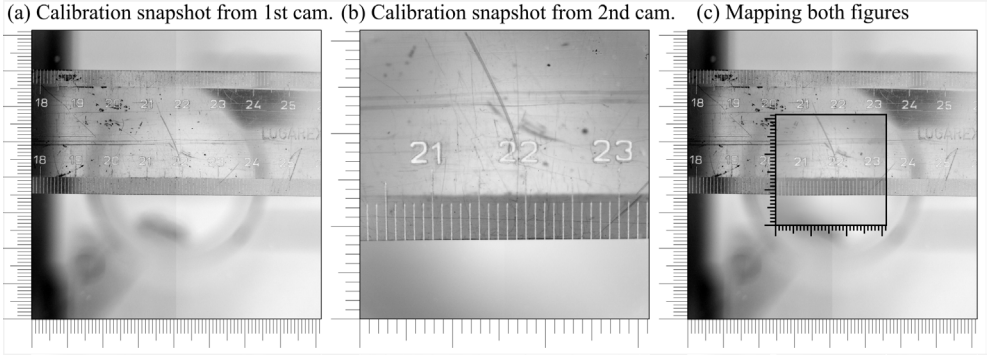

Fig. 1. Calibration snapshots of both cameras (a,b) and together (c).

The PIV method is based on correlating images taken with small time difference ΔT. If ΔT is too long, the correlation peak is too far and the algorithm does not success. On the other hand, if ΔT is small, the velocity calculation works, but the relative uncertainty is higher than it could be. Therefore, it is not useful to use the same ΔT for both FoVs – it would be too

long for the smaller FoV or too short for the larger one. Despite this, we took few snapshots with the same ΔT simultaneously on both cameras in order to check the correspondence of instantaneous structures. The example of instantaneous snapshot taken by both cameras simultaneously is shown in Fig. 2 displaying a reasonable correspondence of the fluctuation velocity structures. The statistical analysis later down uses the data captured separately with different values of ΔT suitable for each FoV.

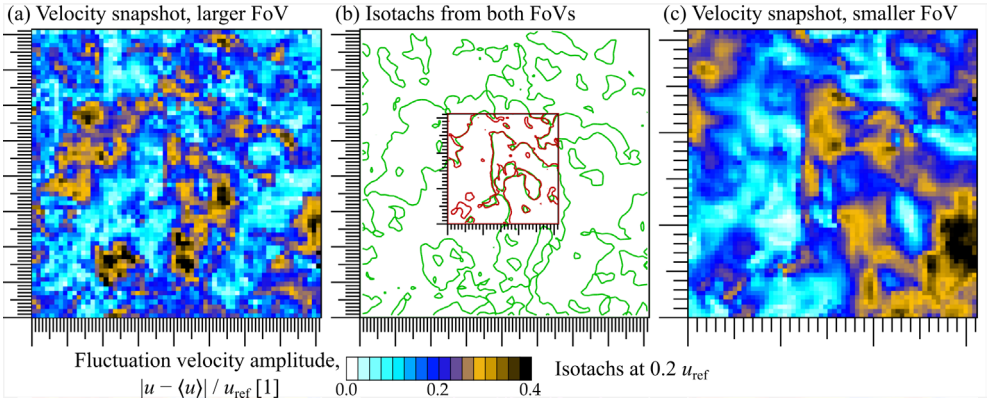

Fig. 2. Example of measured instantaneous velocity fluctuation field. The situation is captured by both cameras simultaneously by applying the same time delay 80 μs, which is too low for the larger FoV and on the edge for the smaller FoV.

3 Results – spectrum, anisotropy and flatness

The spatial spectrum of turbulent kinetic energy is shown in Fig. 3. It is calculated by using our algorithm [8] based on measuring energy of different lengthscale band of Agrawal decomposition [9] [10] [11].

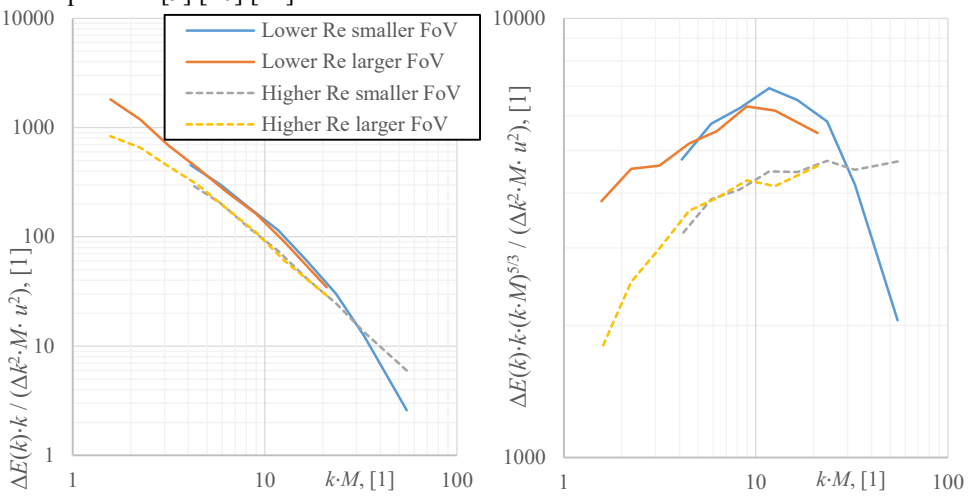

Fig. 3. Left: spatial turbulent kinetic energy spectra as calculated by our algorithm [8]; the wavenumber k is normalized by mesh parameter M and the energy in spatial band by band width Δk, M and velocity u. Right: the same data as in left normalized by the Kolmogorov scaling [12] of inertial range, which would correspond to just a horizontal line in this plot.

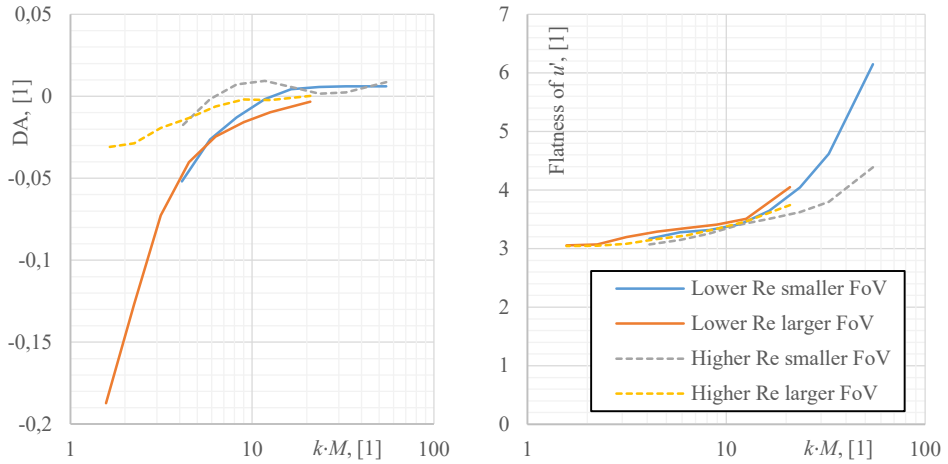

Fig. 4. Left: Degree of anisotropy as a function of wavenumber. Right: Flatness (i.e. fourth statistical moment) of stream-wise velocity fluctuations, note the Gaussian distribution has flatness equal to 3.

It is generally said, that grid turbulence is the best experimental case of Kolmogorov homogenous and isotropic turbulence. However, it is known, that this is not true – the grid turbulence is not homogenous (it evolves with time, i.e. with downstream distance), neither isotropic – the fluctuations are stronger in stream-wise direction. To check the isotropy spectral dependence, we calculate the degree of anisotropy [14] [15] in each lengthscale band as

$$DA = \frac{\sigma_u^2 - \sigma_v^2}{\sigma_u^2 + \sigma_v^2} \tag{2}$$

where σ_u and σ_v are the standard deviations in the stream-wise and perpendicular direction respectively. Fig. 4a shows, that the anisotropy originates at large scales (low k), that the perpendicular fluctuations are stronger than the stream-wise, and that its magnitude is higher at smaller Re.

The flatness or fourth statistical moment of velocity fluctuations describes the relative importance of strong rare events in the flow. It is calculated as

$$F = \frac{\langle u'^4 \rangle}{\sigma_u^4} \tag{3}$$

where u' is the fluctuation part of stream-wise velocity and $\langle \cdot \rangle$ represents ensemble averaging. The "neutral" value of F is 3, because it is flatness of Gaussian distribution. The intermittent effects in turbulence increase this value due to the presence of long-living coherent structures, which are typically of smaller sizes, as it is proven by Fig. 4b. Much more extreme is this effect in quantum turbulence, where the turbulent part of the flow is constructed of quantized vortices of very small size and thus the flatness diverges there [16].

4 Discussion – the vorticity

Vorticity and enstrophy are very interesting quantities in turbulent research [13] [17]. Unfortunately, experimental estimation of vorticity is based on numerical differentiation of the noisy measured velocity field on a grid sampled by the PIV algorithm:

$$\omega_{\mathrm{PIV}}(x,y) = \frac{u(x,y+\Delta y) - u(x,y)}{\Delta y} - \frac{v(x+\Delta x,y) - v(x,y)}{\Delta x} \tag{4}$$

It is only single component perpendicular to the measuring plane; from definition, it cannot catch structures of size of single grid point. Figure 5 shows example of single instantaneous vorticity snapshot captured by both cameras simultaneously. There is a lot of smaller structures visible at the smaller FoV, which are missing in the larger FoV. The limited resolution not only hides small structures, but decreases the amplitude as well.

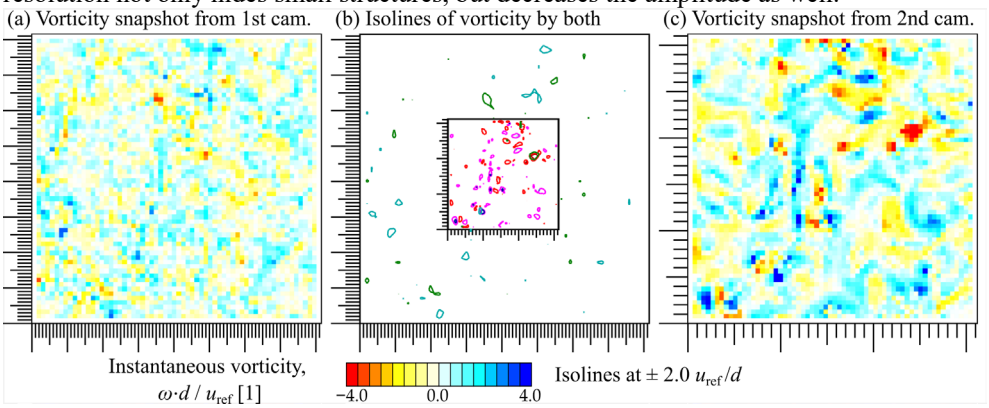

Fig. 5. Example of measured instantaneous vorticity component perpendicular to the measuring area. Note the serious lack of small-scale events in the larger FoV.

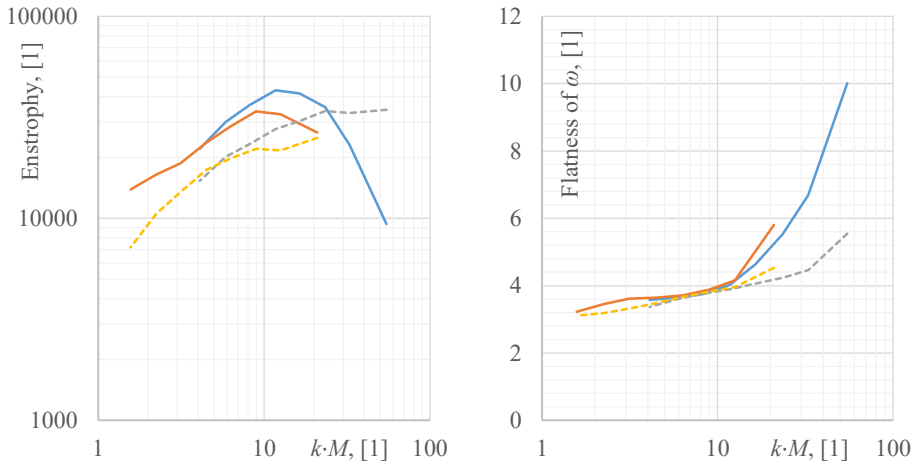

Fig. 6. Left: Estimation of enstrophy spectrum. Note the presented quantity is only rough estimation of enstrophy as it lacks 2 of 3 vorticity components. Additionally, the vorticity is calculated by numerical differentiation on single grid point (different for each FoV), which is probably responsible for the misalignment of the data for smaller and larger FoV. Right: Flatness of the vorticity. The legend is same as in Fig. 3.

Therefore, the enstrophy† estimation is heavily underestimated as well. Note that the presented value is based on one component only. Enstrophy is responsible for energy dissipation, therefore its value grows with wavenumber [13], which is not reproduced by our algorithm [8], additionally, the underestimation depends on the proximity to the PIV grid scale as apparent in Fig. 6. Enstrophy estimation in Fig. 6 is calculated as the variance of vorticity over the FoV and the ensemble and it is normalized as

† *Enstrophy* relates to vorticity analogically, as *turbulent kinetic energy* relates to velocity. Some authors include divergence as well (fully: the determinant of velocity gradient tensor)

$$Z_{\text{estimated}} = \langle \omega^2 - \langle \omega \rangle^2 \rangle \frac{kM}{\Delta k^2 u_{\text{ref}}^2} \tag{5}$$

where the average of vorticity is close zero. Here we hope for some useful comment from reviewer.

Vorticity flatness again shows increasing intermittency towards smaller scales, however, the effect is not trustworthy similarly as the enstrophy estimation although the values between different FoVs rely better. The vorticity flatness increases faster than the velocity flatness with increasing wavenumber. In our resolution, both flatnesses approach to 3 at largest probed scales; we are not sure, how this dependence continued towards larger scales – stay at 3 or go lower?

5 Conclusion

By using two cameras of PIV (particle image velocimetry) system, the lengthscale range has been expanded. The quantities related directly to velocity seem to overlay well, while the derivative quantities, such as vorticity, do not collapse. This decreases the trustworthiness of other results based on vorticity captured with single resolution only [18] [19] [20]. The spectral dependence of degree of anisotropy shows, that the anisotropy originates at larger lengthscales, while the intermittent (strong and rare) events are connected more with smaller lengthscales.

The work was supported from ERDF under project “Research Cooperation for Higher Efficiency and Reliability of Blade Machines (LoStr)” No. CZ.02.1.01/0.0/0.0/16_026/0008389.

References

[1] V. Yanovych, D. Duda, V. Horáček and V. Uruba, "Research of a wind tunnel parameters by means of cross-section analysis of air flow profiles," *AIP Conference Proceedings,* vol. 2189, p. 020024, 2019.

[2] V. Yanovych and D. Duda, "Using ARAMIS system for measurement of structural stability of running wind tunnel," *MATEC Web Conf.,* vol. 328, p. 01003, 2020.

[3] S. Zhang, Handbook of 3D Machine Vision: Optical Metrology and Imaging, Boca Raton: CRC Press, 2013.

[4] T. Kurian and J. H. M. Fransson, "Grid-generated turbulence revisited," *Fluid Dynamics Research,* vol. 41, no. 2, p. 021403, 2009.

[5] S. Usama, J. Tellez-Alvarez, J. Kopec, K. Kwiatkowski, J.-M. Redondo and N. Malik, "Turbulence behind 3D Multi-Scale Sparse Grids," *Journal of Physics: Conference Series,* vol. 1101, p. 012048, 2018.

[6] C. Williamson, "Three-dimensional wake transition," *Journal of fluid mechanics,* vol. 328, pp. 345-407, 1996.

[7] C. Tropea, A. Yarin and J. Foss, Springer Handbook of Experimental Fluid Mechanics, Berlin: Springer, 2007.

[8] D. Duda and V. Uruba, "Spatial spectrum from particle image velocimetry data," *Journal of Nuclear Engineering and Radiation Science,* vol. 5, no. 3, pp. 030912-1-030912-7, 2019.

[9] A. Agrawal and A. Prasad, "Properties of vortices in the self-similar turbulent jet," *Experiments in Fluids,* vol. 33, p. 565–577, 2002.

[10] A. Agrawal, "Measurement of spectrum with particle image velocimetry," *Experiments in Fluids,* vol. 39, p. 836–840, 2005.

[11] D. Duda and V. Uruba, "PIV of air flow over a step and discussion of fluctuation decompositions," *AIP Conference Proceedings,* vol. 2000, p. 020005, 2018.

[12] А. Н. Колмого́ров, "Локальная структура турбулентности в несжимаемой вязкой жидкости при очень больших числах Рейнольдса," *Воспроизводится по ДАН СССР,* vol. 30, p. 299, 1941.

[13] A. Alexakis and L. Biferale, "Cascades and transitions in turbulent flows," *Physics Reports,* Vols. 767-769, no. 12, pp. 1-101, 2018.

[14] I. Solís-Gallego, A. Meana-Fernández, J. Fernández Oro, K. Argüelles Díaz and S. Velarde-Suárez, "Turbulence Structure around an Asymmetric High-," *Journal of Applied Fluid Mechanics,* vol. 10, no. 4, pp. 1013-1027, 2017.

[15] L. Porreca, M. Hollenstein, A. Kalfas and R. Abhari, "Turbulence measurements and analysis in a multistage axial turbine," *Journal of Propulsion and Power,* vol. 23, pp. 227-234, 2007.

[16] M. La Mantia, P. Švančara, D. Duda and L. Skrbek, "Small-scale universality of particle dynamics in quantum turbulence," *Physical Review B,* vol. 94, p. 184512, 2016.

[17] J.-Z. Wu, H.-Y. Ma and M.-D. Zhou, Vorticity and Vortex dynamics, Berlin Heidelberg New York: Springer, 2006.

[18] D. Duda, V. Yanovych and V. Uruba, "An experimental study of turbulent mixing in channel flow past a grid," *Processes,* vol. 8, no. 11, pp. 1-17, 2020.

[19] D. Duda, J. Bém, V. Yanovych, P. Pavlíček and V. Uruba, "Secondary flow of second kind in a short channel observed by PIV," *European Journal of Mechanics, B/Fluids,* vol. 79, pp. 444-453, 2020.

[20] D. Duda, V. Yanovych, V. Tsymbalyuk and V. Uruba, "Effect of Manufacturing Inaccuracies on the Wake Past Asymmetric Airfoil by PIV," *Energies,* vol. 15, no. 3, p. 1227, 2022.

[21] D. Duda, V. Uruba and V. Yanovych, "Wake Width: Discussion of Several Methods How to Estimate It by Using Measured Experimental Data," *Energies,* vol. 14, no. 15, p. 4712, 2021.